Pressure-induced changes in the local structure of $KNbO_3$

Anatoly I. Frenkel, Edward A. Stern, and Yizhak Yacoby

Pressure - Induced Changes in the Local Structure of KNbO$_3$

Anatoly I. Frenkel,* Edward A. Stern[†] and Yizhak Yacoby[‡]

*Materials Research Laboratory,[1]
University of Illinois at Urbana - Champaign, Urbana, Illinois 61801
[†]Department of Physics Box 351560, University of Washington, Seattle, WA 98195,[2]
[‡]Racah Institute of Physics, Hebrew University, Jerusalem, Israel, 91904.[3]

Abstract.
   The local structure of the perovskite KNbO$_3$ at 77 K and 300 K under high pressure, up to 15.8 GPa, has been investigated using the X-ray absorption fine structure (XAFS) technique. We found that local distortions exist throughout the measured range which are peaked off-center at the rhombohedral symmetry sites with a width narrower than the separation between the rhombohedral and orthorhombic sites. On the other hand, diffraction indicates an orthorhombic average structure at 300K, and optical measurements suggest a transition to a cubic phase at high pressures. To explain the difference between pressure - induced changes in KNbO$_3$ structure as measured by XAFS and optical techniques, a pressure - dependent hopping rate in the framework of the eight - site model is proposed.

INTRODUCTION

   Phase transitions in potassium niobate (KNbO$_3$) have been extensively studied, both experimentally and theoretically, since the discovery of its ferroelectric activity in 1949 [1]. Along with other perovskites, KNbO$_3$ has long been considered a classical example of a system undergoing purely displacive phase transitions between three low temperature ferroelectric (FE) phases with different symmetries and a high temperature paraelectric (PE) phase [2].
   The question which transition mechanism, displacive or order-disorder, dominates in a particular ferroelectric, is of central importance. Within a purely displacive model, the atoms in each unit cell vibrate quasi-harmonically about their average positions in the cell. Thus the peak of the position probability distribution

function (PDF) of each atom is at its average position. This means that in the para-electric phase the peak of the PDF is at a centrosymmetric point in the unit cell and at off center position in the ferroelectric (FE) phase. The peak position is expected to be displaced to [100], [110] and [111] directions in the tetragonal orthorhombic and rhombohedral phases, respectively. In contrast, within a pure order-disorder model, the atoms are locally displaced to off-center position in a disordered fashion even in the paraelectric phase. Namely, the atoms vibrate quasi-harmonically about off center positions and may hop among symmetry equivalent off-center positions. The hopping time is long relative to the ordinary quasi-harmonic vibration period even relative to the soft mode period. Below the ferroelectric transition temperature, T_c, the symmetry breaks and the probability of occupying different off-center positions is no longer equal. Thus, within an order-disorder model the PDF has peaks at off-center positions both in the PE and FE phases. In the PE phase the peaks in symmetry equivalent positions have equal intensities. As T decreases below the FE transition, some peaks intensify at the expense of others.

As seen above, the comparison between the local and average structures plays a very important role in our understanding of structural phase transitions. Various experiments provide different kinds of structural information. X-ray and neutron diffraction provide detailed information on the periodic part of the structure. However if one wants to obtain information on local deviations from the average structure one needs to include this possibility explicitly in the data analysis. However, in most cases, the spatial resolution in the pair correlation function provided by this technique is insufficient in order to distinguish between a broad PDF peak at a high symmetry point and a PDF with multiple peaks at off-center positions. Resonant techniques such as NMR and ESR provide local structural information provided the distortions are slow enough to avoid motional narrowing. Thus whenever local structural distortions are observed by these techniques one also obtains an upper limit of the hopping rate. In contrast, if the existence of the local distortions is established by another, faster technique and is not observed by the resonance technique, one can set the lower limit of the hopping rate. In this sense Raman scattering is also a resonance method. If the local distortions are slow compared to a few cm^{-1} the effect of the local distortions will show up either as a violation of the selection rules producing distortion induced first order Raman scattering and/or a central peak. Diffuse X-ray scattering can provide very valuable information on the distortion coherence lengths. Unfortunately these measurements can in certain cases be interpreted in different ways. Finally X-ray Absorption Fine Structure (XAFS) measurements provide local structural information and will detect local deformations even if the hopping rate is almost in the phonon range. Furthermore, the crystal momentum range involved in XAFS experiments ($q = 30\,\text{Å}^{-1}$) is so large that it allows one to determine the pair distance PDF with enough resolution to distinguish between a singly peaked broad PDF and a PDF with multiple peaks at off-center positions. Thus it can be used to determine unequivocally the existence of local structural distortions which cannot be described by quasi-harmonic vibrations.

Temperature has been the most commonly used parameter in a variety of experiments. Hydrostatic pressure has not been often used but it can provide very valuable information. Hydrostatic pressure is known to suppress the ferroelectric phase transition temperatures in perovskite crystals [2]. Although no experimental data is available for $KNbO_3$, it is expected to behave in a way similar to $BaTiO_3$ and obey the modified Curie-Weiss law: $1/\epsilon \propto (P - P_c)$ at constant temperature [2]. If the displacive model holds, the effect of pressure will solely be to change the temperature dependence of the soft mode. On the other hand if the transition is of the order-disorder type or combined displacive and order-disorder it may affect both the off-center displacements in the paraelectric phase and the soft mode. The most suitable method to study the effect of pressure on the off-center displacements is XAFS.

The next Section contains a brief review of previous experimental results in $KNbO_3$. The various experimental results are compared to each other taking into account their different time and length scales. In the following Sections, we report results of XAFS measurements in $KNbO_3$ at 77 K and 300 K and pressures up to 10.2 GPa and 15.8 GPa, respectively. At ambient pressure, the average structure is rhombohedral and orthorhombic, respectively. On the other hand, the experimental XAFS results show that at both temperatures and all the pressures studied, the local structure is rhombohedrally distorted thus supporting the existence of an important element of order-disorder in the pressure-induced phase transitions similar to the one induced by temperature.

REVIEW OF PREVIOUS EXPERIMENTS WITH KNBO$_3$

The properties of $KNbO_3$ at different temperatures and ambient pressure have been thoroughly investigated. The sequence of rhombohedral-orthorhombic-tetragonal-cubic phase transitions in $KNbO_3$ at 263 K, 498 K and 708 K, respectively, was obtained from neutron diffraction experiments [3,4]. Hewat found that the oxygen octahedra vibrate almost as rigid bodies around Nb atoms. The anomalous anisotropy of the oxygen atom mean square displacements has been attributed to the oxygen octahedra librations [4].

Infrared [5], Raman [6], and inelastic neutron scattering [7] experiments, showed that $KNbO_3$ has a transverse optic mode that softens with decreasing temperature. However, the frequency of this mode does not extrapolate to zero at the PE to tetragonal FE phase transition as would be expected in a displacive like model but at a temperature which is hundreds of degrees lower [8]. This result indicates that a simple displacive like model cannot account for the properties of $KNbO_3$.

The Curie-Weiss constant of $KNbO_3$ is about 2.8×10^5 K. This value is consistent with values calculated theoretically for displacive like ferroelectric perovskites and is approximately two orders of magnitude larger than the values calculated in order-disorder like models, thus supporting a displacive model.

Comes, *et al.* [9], observed the existence of X-ray diffuse scattering planes in the reciprocal space of $KNbO_3$, in the orthorhombic, tetragonal and cubic phases. The planes are perpendicular to the [100] type axes. In the cubic phase the only planes missing are the ones that go through the origin. In the lower temperature phases the planes which are not parallel to the vector order parameter disappear. These results have been later confirmed by Holma, *et al.* [10], using synchrotron radiation and electronic detection. Comes, *et al.* [11], proposed that the observed diffuse scattering is due to disordered spontaneous displacements of the Nb atoms in [111] type directions (commonly referred to as the eight-site model). In the paraelectric phase the displacement component in the [100] direction has a relatively long correlation length along the [100] direction and much shorter correlation lengths in the other directions. In the lower temperature phases the correlation lengths along the directions of the order parameter become infinite and the corresponding planes disappear. Later on Comes and Shirane [12] proposed an alternative explanation based on the very flat dispersion of the transverse acoustic phonons along [100] type directions. Holma, *et al.* [10], measured the temperature dependence of the diffuse X-ray scattering and found that the width of the diffuse scattering planes and their intensity vary with temperature. In particular the width seems to extrapolate to zero as T approaches the transition temperature from above. From these results they conclude that a static eight site model cannot account for the observations. They show that their results are consistent with the theoretical quasi harmonic model of Hüller [13] which is qualitatively similar to the alternative suggestion of Comes and Shirane [12]. These models do not require the existence of disorder in the paraelectric phase.

The most direct evidence that Nb atoms are displaced in [111] type directions comes from XAFS experiments. XAFS provides the pair distance PDF between a probe atom and its neighbors. It can be shown that in the quasi-harmonic approximation the interatomic distance PDF would be expected to peak at the average crystal site. The XAFS results show that in both pure $KNbO_3$ [14,15] and in mixed $KTa_xNb_{1-x}O_3$ [16], the Nb-oxygen distance PDF has peaks at distances corresponding to Nb atoms displaced in [111] type directions in all phases including the paraelectric phase.

The existence of local off-center displacements in the paraelectric phase has been recently reproduced theoretically in $KNbO_3$ by molecular-dynamics simulations [17]. The simulation was done in the frame-work of the nonlinear oxygen polarizability model. The order-disorder behavior was observed in the paraelectric phase over several hundred degrees above the FE-PE transition temperature and the inclusion of acoustic phonon coupling led to the correct sequence of phase transitions in this material [17]. Numerous theoretical calculations were carried out in $KNbO_3$ to explain its properties [18–21]. LAPW linear response calculations of the lattice dynamics of cubic $KNbO_3$ by Krakauer, *et al.* [22], succeeded in reproducing the picture of dynamic linear chains directed along the principal cubic axes, thus confirming the eight-site model.

Recently, Girshberg and Yacoby [23] presented a model of ferroelectrics based

on the existence of both a soft mode and spontaneous local off-center ion displacements, and the interaction between the two. Their model accounts quantitatively for both displacive and order-disorder like properties. In $KNbO_3$, for example, their model explains why its Curie-Weiss constant (2.8×10^5 K) is as large as the constant predicted for purely displacive type crystals and at the same time its soft mode does not vanish at T_c but extrapolates to zero at a temperature hundreds of degrees below T_c. They also fully reproduce the temperature and frequency dependence of the imaginary part of the dielectric constant as measured by Vogt [24]. This model also explains the breakdown of the selection rules in the PE phase Raman spectra and the temperature dependence of the diffuse X-ray scattering results. According to this model the eight site off-center displacements are coupled to the soft mode producing a renormalized relaxation mode. As the temperature decreases the relaxation mode slows down and the coherence length increases.

Contrary to temperature dependent measurements, there are only few experiments that studied the effect of pressure on the properties of $KNbO_3$ at room temperature, and almost none that studied them at low temperatures. Recent birefringence and Raman scattering experiments by Gourdain, et al. [25], in the pressure range from 0 to 33 GPa, suggest that $KNbO_3$ undergoes a FE-PE transition at 9 - 10 GPa. The authors describe the structure of the paraelectric phase as cubic and the phase transition as weakly first order. The frequencies of most TO modes soften and their Raman intensity decreases as the transition pressure is approached from below. However, first-order Raman scattering persists in the paraelectric phase all the way up to 33 GPa, the upper limit of the pressure range studied. Other Raman spectroscopy measurements by Shen, et al. [26], reported "three new crystalline phases and an amorphous phase" in the pressure range from 0 to 20 GPa. According to the authors, the displacive phase transitions occur at 2, 6, 9, and 15 GPa, respectively. A phase transition near 2 GPa was obtained by measuring the low frequency dielectric constant under pressure up to 3.2 GPa [27]. X-ray diffraction experiments were performed with $KNbO_3$ under pressure up to 12 GPa by Moya, et al. [28]. No structural transformation was observed in the lattice cell parameters and the structure was characterized as orthorhombic at least up to 12 GPa. The unit cell volume vs pressure behavior was found to be in a good agreement with the Murnaghan equation of state [29]:

$$V = V_0 \left[1 + \left(\frac{B_0' P}{B_0} \right) \right]^{-\frac{1}{B_0'}} , \qquad (1)$$

where V_0 is the volume per unit formula at 300 K, B_0 and B_0' are the isothermal bulk modulus and its pressure derivative, respectively, evaluated at $P = 0$. The best fit of Eq. (1) to the $P - V$ data provided $V_0 = 132.8$ Å^3 and $B_0 = 143$ GPa, in good agreement with the bulk modulus obtained from the dielectric measurements [30]. XAFS experiments with $KNb_{0.87}Ta_{0.13}O_3$ at pressures up to 7.5 GPa and room temperature were recently performed at the Nb K edge [31]. The results showed no changes in the local structure within this pressure range.

The discussion in the preceding paragraph shows that the pressure phase diagram at room temperature is highly controversial. However, almost all authors agree that at least one phase transition does take place at pressures below 15 GPa. The question is whether this transition is reflected in the local structure. In the next section we present the results of our XAFS analysis of the $KNbO_3$ powder which was measured at high pressure and constant temperatures: 77 K and 300 K, where the ambient pressure phases are rhombohedral and orthorhombic, respectively. Besides providing new experimental information on the effect of pressure on the local structure, the low temperature measurement will allow us to compare the effects of pressure in two different phases with (orthorhombic phase) and without (rhombohedral phase) structural disorder.

XAFS ANALYSIS AND RESULTS

Pressure XAFS experiments were performed with $KNbO_3$ powder on the Nb K absorption edge at liquid nitrogen and room temperatures. Details of the sample preparation, experimental setup, synchrotron XAFS measurements and pressure calibration can be found in a separate article [32]. In the present paper, we summarize our modelling procedure which allowed us to solve the local structure around Nb atom within 5 nearest neighbor shells and minimize uncertainties in the obtained parameters.

Data analysis was performed by fitting a theoretical XAFS signal calculated with computer code FEFF6 to the experimental data in r space by Fourier transforming both data and theory. Based on the results of the previous works [14–16,31] we chose the rhombohedrally distorted prototype cubic structure as a model of the local lattice distortion in $KNbO_3$ under pressure. At 77 K, the ambient pressure phase is rhombohedral, therefore this model is a natural choice. At 300 K, the ambient pressure phase is orthorhombic but it is composed of the disordered, locally rhombohedral domains, therefore the same model is a reasonable choice for our data analysis at the both temperatures. Other models, (e.g., orthorhombic distortions) were also tried but the fit quality was much worse than for the rhombohedral model described below.

The independent structural parameters allowed to be varied in the fits to the data at each pressure were the displacements of the oxygen octahedron ($\Delta(O)$) and potassium cube ($\Delta(K)$) in the [111] direction from their positions in the ideal $Pm3m$ perovskite cubic structure, and the isotropic lattice contraction factor $\epsilon = a(P)/a(0)$, where $a(P)$ is the lattice parameter. Hence our model is general enough to accommodate a pure displacive behavior (where Nb atom off-center displacement d vanishes with pressure), a pure order-disorder behavior (where d remains constant under pressure, similar to what was obtained at different temperatures (Ref. [14])), and any combination of these two scenarios.

Five nearest coordination shells around absorbing Nb atom have been analyzed (Fig. 1). Rhombohedral distorted, the oxygen octahedron splits into 2 subshells
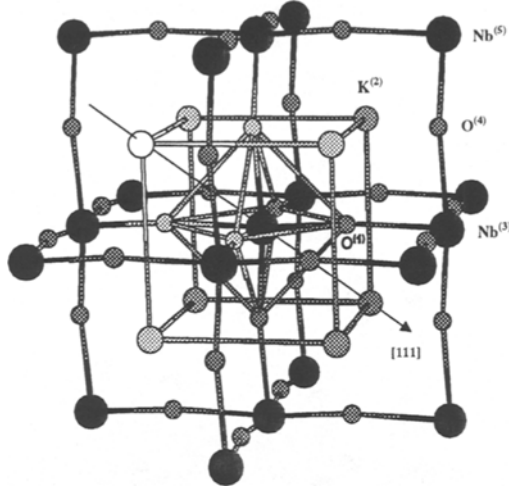
FIGURE 1. Rhombohedral structure of $KNbO_3$. Shown are 5 coordination shells around central Nb atom. Different shades of grey indicate inequivalent $O^{(1)}$ and $K^{(2)}$ sites relative to central Nb.

with 3 atoms each. The potassium cube splits into 4 subshells with 1, 3, 3 and 1 atoms. The 3rd nearest coordination shell consists of 6 niobium atoms. The 4th shell consists of 24 oxygen atoms from neighboring octahedra. They form 4 subshells with 6 atoms each. Finally, the 5th shell consists of 12 niobium atoms.

In our computer program FEFFIT [34], which fits an XAFS theory to the data, physically reasonable constraints between the structural parameters were applied to break their correlations in the fit and reduce the total number of variables.

All the distances R_i between the $Nb^{(0)}$ atom and its i neighbor in each of these 5 shells including inequivalent $O^{(1)}$ and $K^{(2)}$ subshells were expressed as a function of the three independent structural distortion parameters: $\Delta(O)$, $\Delta(K)$ and a lattice contraction factor ϵ using a linear approximation [32].

Effective scattering amplitude of the multiple - scattering photoelectron paths between the central Nb, its neighboring $O^{(1)}$ atoms, and the $Nb^{(3)}$ in the same [100] direction, which are very sensitive to the small deviations from collinearity, were related to $\Delta^2(O)$ via the quadratic term in Taylor expansion.

Besides ϵ, $\Delta(O)$, and $\Delta(K)$, the mean square disorder in the half path length, σ^2, and the muffin-tin energy reference corrections, ΔE_0, were also varied in the non-linear least square fit of theory to data. Additional constraints were applied to relate the σ^2 and ΔE_0 of the multiple scattering paths to the single scattering paths connecting the same atoms [32].

Numerical results for $\Delta(O)$, the lattice parameter a and the Nb off-center displacement d relative to the oxygen octahedra at all pressures measured at 77 K and 300 K, respectively, have been reported in Ref. [32]. The values of $\Delta(K)$ and the $Nb^{(0)}$-$K^{(2)}$ σ^2 are comparable to the uncertainties at all pressures and temperatures,
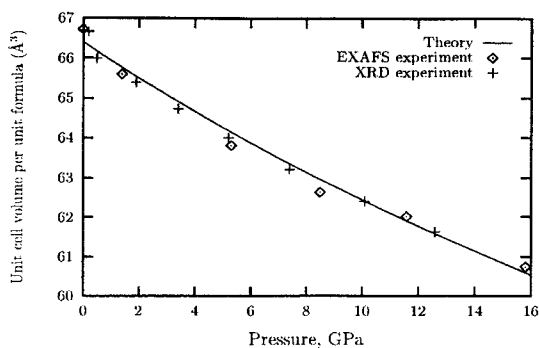
FIGURE 2. Unit cell volume per unit formula vs pressure at 300 K (symbols) calculated from the lattice parameter determined by XAFS (this work) and XRD (Ref. [28]) Solid line shows the behavior predicted by theory (Ref. [29]). Uncertainties in the experimental data are smaller than the symbols and are not shown.
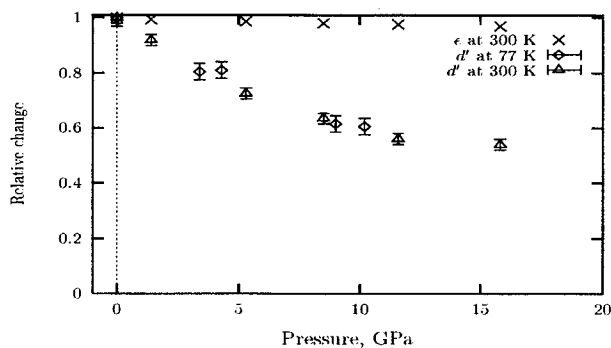
FIGURE 3. Changes in lattice parameter (at 300 K), Nb off-center displacements at 77 K and 300 K, normalized by their values at ambient pressure and respective temperatures.

and are, therefore, omitted.

The pressure dependence of the unit cell volume per unit formula calculated using the obtained $Nb^{(0)}$-$Nb^{(3)}$ distances (see Discussion Section) are shown in Fig. 2. The pressure dependent, Nb off-center displacements $d'(P) = d(P)/d(0)$ normalized to ambient pressure are shown in Fig. 3 for both 77 K and 300 K, along with the normalized unit cell dimension $\epsilon(P) = a(P)/a(0)$ measured at room temperature.

Mean square relative deviations of the distances between the $Nb^{(0)}$ atom and its 1st, 3rd, 4th and 5th NN have been reported in Ref. [32] for all temperatures and pressures. We obtained that σ^2 of the nearer neighbor pairs $Nb^{(0)}$ - $O^{(1)}$ and $Nb^{(0)}$ - $Nb^{(3)}$ decrease with pressure as expected. σ^2 of the longer $Nb^{(0)}$-$O^{(4)}$ and $Nb^{(0)}$ - $Nb^{(5)}$ pairs, however, have a completely different trend. These σ^2 increase with pressure at both temperatures. This indicates that pressure increases the oxygen octahedra librations and distortions, and decreases the Nb displacement -

245

displacement correlation length [32].

DISCUSSION

Before discussing the new experimental results obtained for the Nb off-center displacements under pressure, we describe several important cross-checks made between our results and those obtained by other techniques.

The ambient pressure Nb off-center displacements along [111] obtained at 77 K with XAFS [32], are in good agreement with the 0.218 Å displacement measured at 230 K by neutron diffraction [4]. Although the XAFS and diffraction techniques generally measure different structures (XAFS measures local relative atomic positions while diffraction measures the average crystal structure), at this temperature, the rhombohedral structure of $KNbO_3$ is ordered, and the results of these two techniques should agree with each other. The fact that we obtained the same displacement as neutron diffraction, is, therefore, expected, and adds confidence to our other results.

Another important cross-check is the behavior of the unit cell volume with pressure. It is known from the X-ray diffuse scattering results [35,9] that the off-center displacements of the $Nb^{(0)}$ and its nearest neighbor $Nb^{(3)}$ atoms strongly correlate in [100] cubic directions. Eight nearest neighbor Nb atoms (in [100] directions) define the prototype cubic cell (the rhombohedral angle is 89.93° (Ref. [4]) and its deviation from 90° can be neglected). The local disorder of Nb displacements should not distort the rigid cubic frame of the neighboring Nb atoms due to the [100] correlations between their displacements. The small value of σ^2 between the $Nb^{(0)}$ and $Nb^{(3)}$ atoms as measured by XAFS confirms this high correlation. The volume of the unit cell per formula, therefore, can be approximated as cube of the distance between $Nb^{(0)}$ and $Nb^{(3)}$ atoms, obtained in our XAFS analysis for all pressures: $V_{XAFS} = R^3$. The average unit cell volume per formula, V_{XRD}, measured by X-ray diffraction, is expected to be equal to V_{XAFS} in this case. The plot of the $P - V$ data (Fig. 2) for V_{XAFS} (this work) and V_{XRD} (Ref. [28]) demonstrates that these pressure behaviors of the unit cell volume, independently measured by XAFS and X-ray diffraction, are indeed in a very good agreement with each other and with Eq. (1).

We obtained that, at ambient pressure, the direction of the Nb displacements of almost the same magnitude in both orthorhombic and rhombohedral phases remains along the [111] cubic axis thus confirming previous XAFS results [14–16]. This indicates that the local structure unit cells in the orthorhombic phase of $KNbO_3$ retain their rhombohedral distortions. The fact that the X-ray diffraction (XRD) measures the structure of $KNbO_3$ at room temperature as orthorhombic does not contradict but complements our XAFS results. Since XRD is a fast measurement, with the same time scale as XAFS ($\approx 10^{-15}$ s), the difference between the two results should be attributed to a small correlation length of the Nb atom [111] displacements. As follows from the analysis of the behavior of σ^2 of the

$Nb^{(0)}$-$Nb^{(5)}$ bonds, high pressure decreases the already small correlation length even further [32]. Diffraction averages over the disorder of the local unit cells to obtain the orthorhombic phase.

It is worth noting that in this study we obtained that the distribution function of the $Nb^{(0)}$-$O^{(1)}$ distances remains convincingly peaked off the center of the first neighbor oxygen octahedron along the [111] directions for all temperatures and pressures since the displacement of the peak persists to be about three times the corresponding vibrational amplitude σ of the $Nb^{(0)}$-$O^{(1)}$ bonds [32]. Because of the good spatial resolution of the XAFS data (0.04 Å in our case), and small uncertainties in both the Nb-$O^{(1)}$ distances (0.01 Å, or better) and σ^2 (0.0010 - 0.0016 Å^2), it is possible to distinguish this off center distribution, characteristic of a multi-well potential, from a single-well anisotropic vibration peaked about the center which has its largest displacement along the [111] directions. It is also possible to distinguish between the [111] (rhombohedral) and [110] (orthorhombic) directions of the local Nb displacements, since our spatial resolution is much better than the 0.11 Å required. To verify this we checked a fit to the model with orthorhombic distortions. As expected the fit quality was clearly significantly worse than for the rhombohedral model. Unless the measurement has sufficient spatial resolution it is not possible to make this distinction. For example, this distinction could not be made in measurements of $KNbO_3$ [4] and $PbTiO_3$ [36] using the neutron diffraction technique.

In disagreement with our XAFS results, Shuvaeva, *et al.* [37,38], using polarized XAFS and X-ray diffraction measurements of the single crystal $KNbO_3$ at room temperature, obtained that the direction of the local Nb atom off-center displacement agrees closely with the direction of the [110] polar axis in the orthorhombic phase. The error analysis, however, was not performed. The quality of the fits reported in Ref. [37] indicates that the uncertainties in the obtained parameters (due to noise in the data or lack of spatial resolution) may have been too large to convincingly discriminate between the [110] and [111] directions of Nb atom displacements.

As to the pressure effects, where a displacive transition to the cubic phase at 9 - 10 GPa has been proposed from the birefringence and Raman spectroscopy results [25,26] from the fact that those effects vanish or become small above 9 - 10 GPa [25], XAFS measurements show conclusively that the local distortions do not vanish. As Fig. 3 demonstrates, the Nb displacement does not vanish but remains fixed in direction and changes continuously through the 9 - 10 GPa region with no visible slope change.

This apparent contradition between the two local probes of XAFS and Raman can be reconciled by taking into account the different time scales of the optical and x-ray measurements as discussed in Sects. I and II. In the eight-site model [11] the local displacements are in the [111] directions as XAFS observes. However, these local displacements become progressively more disordered as $KNbO_3$ transforms from the rhombehedral to the orthorhombic, tetragonal, and then completely disordered

in the cubic phase. These disordered regions are small enough to average out in diffraction and birefrigence measurements which probe over relatively larger dimensions. To account for the difference between the two local probes (Raman and XAFS) the dynamics of the disordering must be considered. At room temperature and below 9 - 10 GPa the hopping time of the Nb atoms between equivalent [111] sites is longer than the lifetime of the Raman measurement and Raman senses the displacement. However, above 9 -10 GPa the hopping lifetime becomes shorter than the lifetime of the Raman measurement which then senses the average over the disordered [111] sites, giving higher symmetry and a weaker first order line. The XAFS measure is always much faster than any hopping time and always senses the local displacement. The theory of Girshberg and Yacoby [23] demonstrated that a temperature - dependent hopping rate among equivalent off-center positions is a crucial element in giving a quantitative explanation of the properties of the temperature - induced FE-PE transitions in $KNbO_3$.

What remains to explain is the cause of the increase of the hopping rate with increasing pressure. The hopping rate ν is given by $\nu = \nu_0 e^{-u/k_B T}$ where ν_0 is some attempt frequency, u is the barrier height between equivalent sites, and k_B is the Boltzmann constant. Since T is constant, the increase in ν must occur because of a decrease of u with pressure. As Fig. 3 shows, pressure has two effects: to decrease slightly the lattice constant and to decrease much more the displacement d. Decreasing the lattice constant would be expected to increase u. However, the much larger concomitant decrease of d should decrease u because it decreases the distance required to hop to neighboring equivalent sites. For example the barrier vanishes when $d = 0$. It is reasonable to expect that the much greater change in d would dominate, explaining the increased rate of hopping with increasing pressure.

The measured decrease of the local distortion d with increasing pressure can be understood theoretically using the pseudo Jahn-Teller distortion ideas of Bersuker [39]. As Bersuker has shown, d depends inversely on the energy gap between the ground and excited states coupled by the distortion. With the decreasing lattice constant with increasing pressure the splitting of the excited states will increase exponentially because of the corresponding increase in overlap of neighboring atom wave-functions, explaining the greater rate of decrease of d compared to that of the lattice constant as shown in Fig. 3.

CONCLUSIONS

Nb K-edge XAFS data of $KNbO_3$ were measured at 77 K and 300 K under high pressure, up to 15.8 GPa. We observed a pressure-induced gradual displacement of Nb atom towards the center of oxygen octahedra at both temperatures, 77 K and 300 K. The Nb off-center displacements are in the [111] type directions at all temperatures and pressures, in spite of the fact that the crystal has different crystallographic structures.

Our results show, that, while the average structure reportedly exhibits one or

more pressure-induced phase transitions, the local structure remains rhombohe-
drally distorted at all pressures up to 15.8 GPa, indicating a significant order -
disorder element in the phase transitions.

The difference between XAFS and other relevant experimental techniques as
a function of pressure is explained by their different spatial resolution, time and
length scales. To reconcile these differences it is concluded that the hopping rate
of Nb atoms among their equivalent sites increases with increasing pressure due to
the concomitant relatively large decrease in the Nb displacements.

ACKNOWLEDGEMENTS

REFERENCES

1. Matthias B. T., *Phys. Rev. B* **75**, 1771 (1949).
2. Lines M. E. and Glass A. M., *Principles and Applications of Ferroelectrics and Related Materials*, Oxford: Clarendon Press, 1977.
3. Perry C. H., Hayes R. R., Tornberg N. E., *Proceedings of the International Conference on Light Scattering of Solids*, Ed. M. Balkanski.
4. Hewat A. W., *J. Phys. C: Solid State Phys.*, **6**, 2559 (1973).
5. Fontana M. D., Metrat G., Servoin J. L., and Gervais F., *Ferroelectrics* **38**, 797 (1981).
6. Fontana M. D., Kugel G. E., Vamvakas J., and Carabatos C., *Solid State Commun.*, **45**, 873 (1983).
7. Fontana M. D., Dolling G., Kugel G. E., and Carabatos C., *Phys. Rev. B* **20**, 3850 (1979).
8. Fontana M. D., Metrat G., Servoin J. L., and Gervais F., *J. Phys. C* **16**, 483 (1984).
9. Comes R., Lambert M., and Guiner A., *Acta. Cryst.*, **A26**, 244 (1970).
10. Holma M., Takesue N., and Chen H., *Ferroelectrics* **164**, 237 (1995).
11. Comes R., Currat R., Denoyer F., Lambert M. and Quittet A. M., *Ferroelectrics* **12**, 3 (1976).
12. Comes R. and Shirane G., *Phys. Rev. B* **5**, 1886 (1972).
13. Hüller A., *Solid State Commun.*, **7**, 589 (1969).
14. Kim K. H., Elam W. T., and Skelton E. F., *Mat. Res. Soc. Symp. Proc.*, **172**, 291 (1990).
15. Mathan N., Prouzet E., Husson H., and Dexpert H., *J. Phys.: Condens. Matter* **5**, 1261 (1993).
16. Hanske-Petitpierre O., Yacoby Y., Mustre de Leon J., Stern E. A., and Rehr J. J., *Phys. Rev. B* **44**, 6700 (1991).

17. Sepliarsky M., Stachiotti M. G., and Migoni R. L., *Phys. Rev. B* **56**, 566 (1997); Stachiotti M. G., Sepliarsky M., Tinte S., Migoni R. L., and Rodrigues C. O., Proceedings of the Fifth Williamsburg Worskhop on First-Principles Calculations for Ferroelectrics, Williamsburg, VA, 1998.

18. Yu R. and Krakauer H., *Phys. Rev. Lett.*, **74**, 4067, (1995); Krakauer H., Yu R., Wang C.-Z., Rabe K., and Waghmare U. V., Proceedings of the Fifth Williamsburg Worskhop on First-Principles Calculations for Ferroelectrics, Williamsburg, VA, 1998.

19. Kvyatkovskii O. E., *Phys. Solid State* **39**, 602 (1997).

20. Dorfman S., Fuks D., Gordon A., Postnikov A. V., and Borstel G., *Phys. Rev. B* **52**, 7135 (1995).

21. Bussmann-Holder A., *J. Phys. Chem. Solids* **57**, 1445 (1996).

22. Krakauer H., Yu R., and Wang C. Z., *J. Phys. Chem. Solids* **57**, 1409 (1996).

23. Girshberg Ya. and Yacoby Y., *Solid State Commun.*, **103**, 425 (1997).

24. Vogt H., *Phys. Rev. B* **51**, 8046 (1995).

25. Gourdain D., Moya E., Chevrin J. C., Canny B., and Pruzan Ph., *Phys. Rev. B* **52**, 3108 (1995).

26. Shen Z. X., Hu Z. P., Chong T. C., Beh C. Y., Tang S. H., and Kuok M. H., *Phys. Rev. B* **52**, 3976 (1995).

27. Errandonea D. and Moya E., *Phys. Stat. Sol. (B)* **203**, R1 (1997).

28. Moya E., Tinoco T., Polian A., and Itie J. P., *Ferroectric Letters* **22**, 59 (1997).

29. Murnaghan F. D., *Am. J. Math.*, **49**, 235 (1937).

30. Wiesendanger E., *Ferroelectrics* **6**, 263 (1974).

31. Wang F., Ravel B., Yacoby Y., Stern E. A., and Ingalls R., *J. Phys. IV* **7**, C2-1225 (1997).

32. Frenkel A. I., Wang F. M., Kelly S., Ingalls R., Haskel D., and Stern E. A., *Phys. Rev. B* **56**, 10869 (1997).

33. Zabinsky S. I., Rehr J. J., Ankoudinov A., Albers R. C., and Eller M. J., *Phys. Rev. B* **52**, 2995 (1995).

34. Stern E. A., Newville M., Ravel B., Yacoby Y., and Haskel D., *Physica B* **208 & 209**, 117 (1995).

35. Comes R., Lambert M., and Guiner A., *Solid State Commun.*, **15**, 715 (1974).

36. Nelmes R. J. and Kuhs W. F., *Solid State Commun.*, **54**, 721 (1980); Nelmes R. J., Piltz R. O., Kuhs W. F., Tun Z., and Restori R., *Ferroelectrics* **108**, 165 (1990).

37. Shuvaeva V. A., Yanagi K., Sakaue K., and Terauchi H., *J. Phys. Soc. Japan* **66**, 1351 (1997).

38. Shuvaeva V. A. and Antipin M. Y., *Crystallography Reports* **40**, 466 (1995).

39. Bersuker I. B. and Polinger V. Z., *Vibronic Interactions in Molecules and Crystals*, Springer Series in Chemical Physics, Vol. 49, New York: Springer, 1989.